Mst1/2 Kinases Inhibitor, XMU-MP-1, Attenuates Angiotensin II-Induced Ascending Aortic Expansion in Hypercholesterolemic Mice

Michihiro Okuyama, MD, PhD; Weihua Jiang, BSc;
Lihua Yang, BSc; Venkateswaran Subramanian, PhD

Background: Ascending and abdominal aortic aneurysms (AAs) are asymptomatic, permanent dilations of the aorta with surgical intervention as the currently available therapy. Hippo-Yap signaling cascade plays a critical role in stem cell self-renewal, tissue regeneration and organ size control. By using XMU-MP-1, a pharmacological inhibitor of the key component of Hippo-Yap signaling, MST1/2, we examined the functional contribution of Hippo-Yap in the development of AAs in Angiotensin II (AngII)-infused hypercholesterolemic mice.

Methods and Results: MST, p-MST, p-YAP, p-MOB and TAZ proteins in AngII-infused ascending and abdominal aortas were assessed by immunohistochemical and western blot analyses. To examine the effect of MST1/2 inhibition on AAs, western diet-fed low density lipoprotein (LDL) receptor –/– mice infused with AngII were administered with either vehicle or XMU-MP-1 for 5 weeks. Hippo-YAP signaling proteins were significantly elevated in AngII infused ascending and abdominal aortas. XMU-MP-1 administration resulted in the attenuation of AngII-induced ascending AAs without influencing abdominal AAs and aortic atherosclerosis. Inhibition of Hippo-YAP signaling also resulted in the suppression of AngII-induced matrix metalloproteinase 2 (MMP2) activity, macrophage accumulation, aortic medial hypertrophy and elastin breaks in the ascending aorta.

Conclusions: The present study demonstrates a pivotal role for the Hippo-YAP signaling pathway in AngII-induced ascending AA development.

Key Words: Angiotensin II; Ascending aortic dilation; MST1/2; XMU-MP-1; YAP

Ascending and abdominal aortic aneurysms (AAs) are life-threatening permanent dilations of the aorta, mediated by totally different etiologies and have highly distinct pathologies.[1,2] Ascending AAs are strongly associated with genetic abnormalities of connective tissues.[3] Abdominal AAs are positively associated with aging, smoking, and male gender, with relatively weak genetic associations.[4] Both ascending and abdominal AAs are asymptomatic, and the current therapy mainly relies on surgical intervention.

Infusion of Angiotensin II (AngII), a bioactive peptide of the renin-angiotensin system, into hypercholesterolemic mice promotes ascending and abdominal AAs in addition to atherosclerosis. However, the underlying pathologies of AngII-induced ascending and abdominal AAs are distinct.[5,6] For instance, the AngII-induced abdominal AAs are characterized by small focal regions of leukocyte accumulation in the medial layer of the aorta. In contrast, the

AngII-induced ascending AAs are characterized by leukocyte accumulation predominantly on the adventitial side of the aorta.[5] Currently, the underlying mechanisms and identification of key players in the development of AngII-induced aortic vascular pathologies remain poorly understood.

Mammalian sterile 20-like kinases, MST1 and MST2 (MST1/2), are key components of the Hippo-Yap signaling cascade that play a critical role in stem cell self-renewal, tissue regeneration, and organ size control.[7–9] The Hippo-YAP signaling pathway is a cascade of kinases formed by MST1/2; a scaffolding protein, Salvador (Sav); nuclear Dbf2-related family kinases, LATS1 and LATS2 (LATS1/2); and an adaptor protein, MOB1. MST1/2 phosphorylates and activates the LATS1/2-MOB1 complex, which in turn phosphorylates YAP. Phospho-YAP is either sequestered in the cytoplasm by 14-3-3 protein or degraded. When the Hippo pathway is not active, YAP translocates to the nucleus and forms a functional hybrid with a transcriptional

enhancer factor A (TEA) domain transcription factor to turn on pro-survival and proliferative genes.[7–9] In mice, genetic alterations in the Hippo-YAP signaling cascade resulted in sustained tissue growth.[10,11] Recently, in ascending AA patients, a substantial reduction of YAP in the aortic media has been reported.[12] However, the functional role of Hippo-YAP in ascending and abdominal AA development is unknown. Understanding the physiological function of Hippo-YAP during AA development would yield a novel insight into AAs mechanisms.

Using a pharmacological inhibitor of MST1/2, we examined the relative contribution of Hippo-YAP signaling to the development of AngII-induced ascending and abdominal AAs. 4-((5,10-dimethyl-6-oxo-6,10-dihydro-5H-pyrimido[5,4-b] thieno[3,2-e] [1,4]diazepin-2-yl)amino) benzenesulfonamide or XMU-MP-1, is a potent and selective inhibitor of MST1/2.[13,14] By using XMU-MP-1, our findings demonstrate a functional role of Hippo-YAP signaling in the development of ascending, not abdominal, AAs in hypercholesterolemic mice.

Methods

Mice
Both LDL receptor −/− (stock # 002207) and C57BL/6J (Stock# 000664) mice were purchased from The Jackson Laboratory (Bar Harbor, ME, USA). LDL receptor −/− mice were backcrossed 10-fold into a C57BL/6 background. Age-matched male littermates (8–10 weeks old) were used for the present study. Mice were maintained in a barrier facility and fed normal mouse laboratory diet. All study procedures were approved by the University of Kentucky Institutional Animal Care and Use Committee (Protocol # 2011-0907). This study followed the recommendations of The Guide for the Care and Use of Laboratory Animals (National Institutes of Health).

Diet
To induce hypercholesterolemia, mice were fed a diet supplemented with saturated fat (21% wt/wt milk fat and 0.15% cholesterol; TD.88137, Harlan Teklad, Indianapolis, IN, USA) for 5 weeks.[15]

MST1/2 Inhibitor, XMU-MP-1, Administration
XMU-MP-1 (Cat # 22083) was purchased from Cayman chemicals, Ann Arbor, MI, USA. The XMU-MP-1 compound was dissolved in dimethyl sulfoxide at a concentration of 30 mg/mL and administered daily by gavage at a dose of 3 mg/kg/day for different intervals of time ranging from 7 to 35 days.

AngII Infusion
After an initial week of western diet feeding, mice were implanted with Alzet osmotic minipumps (model 2004; Durect Corporation, Cupertino, CA, USA), subcutaneously into their right flanks, and infused with either saline or AngII (1,000 ng/kg/min; Bachem, Torrance, CA, USA) continuously for a period of 7 or 28 days, as described previously.[16,17] Mice were fed a western diet throughout the infusion study.

Blood Pressure Measurement
Systolic blood pressure (SBP) was measured non-invasively on conscious mice by volume pressure recording of the tail using a computerized tail cuff blood pressure system (Kent Scientific Corp, Torrington, CT, USA).[18] SBP was measured on 3 consecutive days prior to pump implantation, and during the last 3 days of AngII infusion.

Measurement of Plasma Components
Plasma cholesterol concentrations were measured using a commercially available enzymatic kit (Wako Chemicals, Richmond, VA, USA) as described previously.[15]

Ultrasound Imaging of Abdominal AAs
Luminal dilation of the abdominal aorta was measured by using a high frequency ultrasound imaging system (Vevo 2100; Visual Sonics, Toronto, Canada) using a MS400 MicroScanTM transducer with a resolution frequency of 18–38 MHz.[16,17] Mice were anesthetized and restrained in a supine position to acquire ultrasonic images. Short axis scans of abdominal aortas were performed from the left renal arterial branch level to the suprarenal region.[16,17] Images of abdominal aortas were acquired and measured to determine maximal diameter in the suprarenal region of the abdominal aorta. Aortic images were acquired at day 0 and 28 of AngII-infusion.

Quantification of Atherosclerosis, Ascending and Abdominal AAs
After saline perfusion through the left ventricle of the heart, aortas were removed from the origin to iliac bifurcation, and placed in formalin (10% wt/vol) overnight. Adventitial fat was cleaned from the aortas. Atherosclerosis was quantified on aortic arches and thoracic aorta as lesion area, and percent lesion area on the intimal surface by en face analysis, as described previously.[15,19] Lesion areas were measured using Image-Pro Plus software (Media Cybernetics, Bethesda, MD, USA) by direct visualization of lesions under a dissecting microscope. Abdominal AA measurements were quantified ex vivo by measuring the maximum external width of the suprarenal abdominal aortic diameter using computerized morphometry (Image-Pro Cybernetics, Bethesda, MD, USA), as described previously.[16,20] For ascending AA measurement, aortas were cut open longitudinally from the inner arch curvature to the iliac bifurcation, as well as from the outer curvature to the subclavian branch. Aortas were pinned and photographed using a Nikon Digital Camera (DXM1200). Intimal areas of ascending aortas were measured from the ascending aorta to the subclavian branch using Image-Pro Plus software.[16,21]

Tissue Histology
Ascending and abdominal aortas were placed in optimal cutting temperature and sectioned (10-μm thickness/section) in sets of 10 slides serially with 9 sections/slide by using a cryostat. One of the slides was stained with Verhoeff's Iron Hematoxylin staining and measurements were performed to determine medial thickness and elastin breaks. To quantify medial thicknesses, every section from each slide was measured perpendicular from internal to external elastic lamina. Immunohistochemical staining was performed on AA sections to detect phospho YAP and YAP using the rabbit anti-mouse phospho-YAP (Ser127; D9W21, catalog No: 13008, 1:500) and YAP (D24E4; 1:200, catalog No: 8418, 1:200) antibodies (Cell Signaling Technology [CST], Danvers, MA, USA). The following reagent was used to detect macrophages: rat anti-mouse CD68 (1:200, catalog No. MCA1957; Bio-Rad, Hercules, CA, USA).
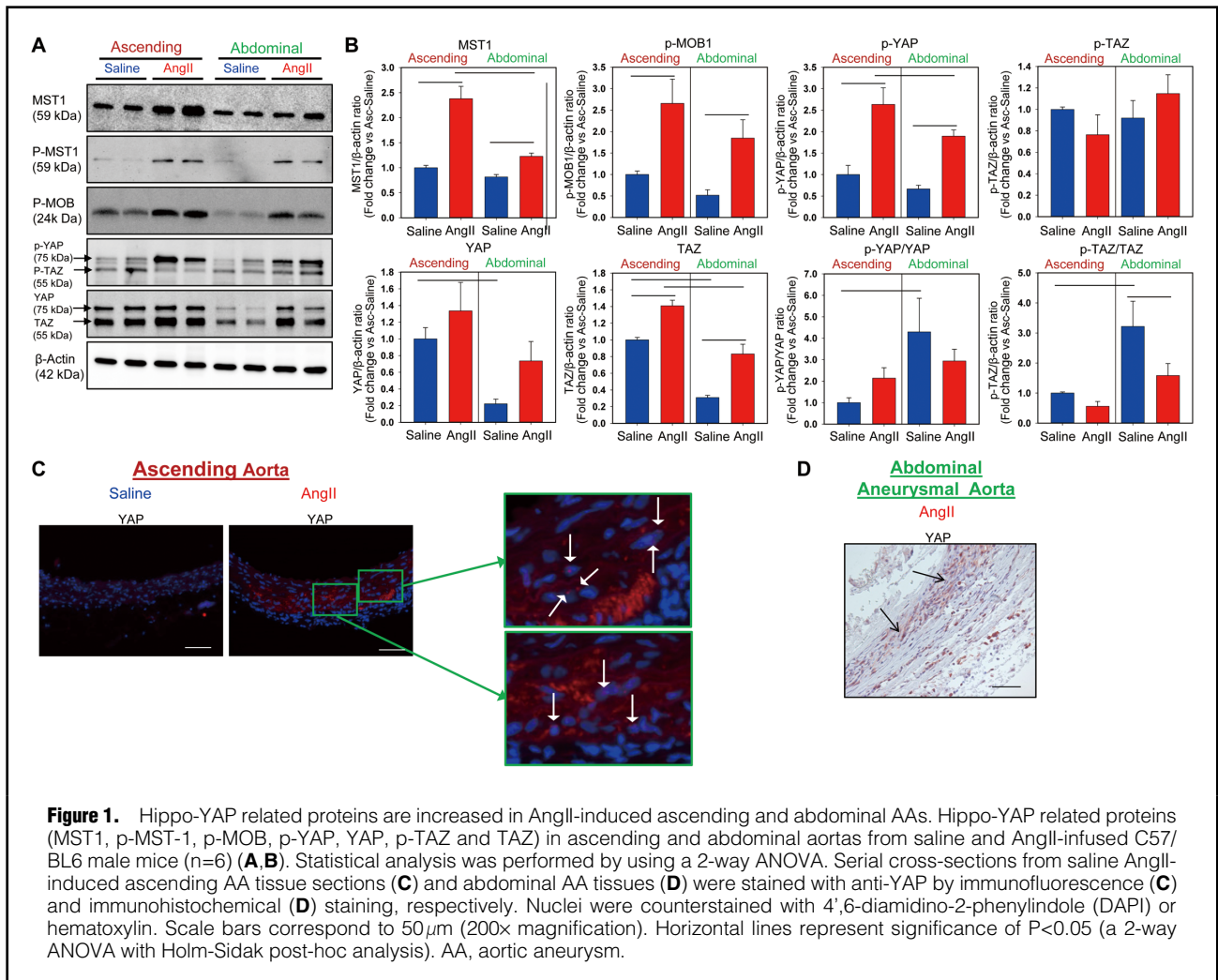
Figure 1. Hippo-YAP related proteins are increased in AngII-induced ascending and abdominal AAs. Hippo-YAP related proteins (MST1, p-MST-1, p-MOB, p-YAP, YAP, p-TAZ and TAZ) in ascending and abdominal aortas from saline and AngII-infused C57/BL6 male mice (n=6) (**A,B**). Statistical analysis was performed by using a 2-way ANOVA. Serial cross-sections from saline AngII-induced ascending AA tissue sections (**C**) and abdominal AA tissues (**D**) were stained with anti-YAP by immunofluorescence (**C**) and immunohistochemical (**D**) staining, respectively. Nuclei were counterstained with 4',6-diamidino-2-phenylindole (DAPI) or hematoxylin. Scale bars correspond to 50 μm (200× magnification). Horizontal lines represent significance of P<0.05 (a 2-way ANOVA with Holm-Sidak post-hoc analysis). AA, aortic aneurysm.

Immunostaining was performed on formalin-fixed frozen or paraffin-embedded sections, with appropriate negative controls, as described previously.[15,22]

Immunofluorescence

Immunofluorescence staining on ascending aortic sections were performed on formalin-fixed frozen sections to detect phospho YAP and YAP using the rabbit anti-mouse phospho-YAP (Ser127; D9W21, catalog No: 13008, 1:500) and YAP (D24E4; 1:200, catalog No: 8418, 1:200) antibodies (CST, Danvers, MA, USA). The positive staining was visualized as red color using fluorescent anti-rabbit secondary fluorescent antibodies (Alexa Fluor Plus 594, catalog No: A32754; Thermo Fisher Scientific, Waltham, MA, USA). Nuclei were co-stained using mounting media containing 4',6-diamidino-2-phenylindole (DAPI) reagent (Fluoroshield with DAPI, catalog No: F6057, Millipore Sigma, Burlington, MA, USA).

Nuclei Staining

Frozen sections were fixed in ice-cold acetone and permeabilized with 0.5% Triton X-100 for 5 min at room temperature. Sections were then mounted with mounting media containing DAPI reagent Fluoroshield with DAPI (catalog No: F6057; Millipore Sigma, Burlington, MA, USA). Nuclei

counts were quantified on 4 aortic segments of equivalent length (0.25 mm) per groups of mice using fluorescent microscope-captured images.

Western Blot Analyses

Ascending and abdominal aortic tissue lysates were extracted in radioimmunoprecipitation assay lysis buffer, and protein content was measured using a Bradford assay (Bio-Rad). Protein extracts (20–30 μg) were resolved by using sodium dodecyl sulfate-polyacrylamide gel electrophoresis (SDS-PAGE) (6.0 or 7.5% wt/vol) and transferred electrophoretically to polyvinylidene difluoride (PVDF) membranes (Millipore). After blocking with non-dry fat milk (5% wt/vol), membranes were probed with primary antibodies. The following antibodies were used: MST1 (CST, catalog No: 3682), Phospho-MST1 (Thr183) (CST, catalog No: 3681), Phospho-MOB1 (Thr35) (D2F10) (CST, catalog No: 8699), Phospho-YAP (Ser127) (D9W2I) (CST, catalog No: 13008), YAP/TAZ (D24E4) (CST, catalog No: 8418). Membranes were incubated with appropriate horseradish peroxidase (HRP)-labeled secondary antibodies. Immune complexes were visualized by using chemiluminescence (Pierce, Rockford, IL, USA) and quantified using a Bio-Rad Imager.

Zymography

Aortic protein extracts (5 mg) were resolved under non-reducing conditions by sodium dodecyl sulfate polyacrylamide gel electrophoresis (10% wt/vol), polymerized in the presence of gelatin (2 mg/mL) to measure the activities of matrix metalloproteinase (MMP) 2 and 9. Gels were washed with Triton X-100 (2.5% vol/vol) and distilled water for 30 min each. Gels were then incubated overnight at 37°C in Tris buffer containing calcium chloride (5 mmol/L) and sodium azide (0.02% wt/wt), pH 8.0 for MMP2/MMP9. After incubation, gels were stained with Coomassie Brilliant Blue followed by destaining with acetic acid (7% vol/vol) and methanol (40% vol/vol). Gel images were captured using a Bio-Rad Imager, and the unstained, translucent, digested regions represented areas of MMP activity.[17]

Statistical Analyses

Data are represented as mean±SEM. Statistical analyses were performed using by SigmaPlot 14.0 (SYSTAT Software Inc., San Jose, CA, USA). Repeated measurement data were analyzed with statistical analysis software (SAS) fitting a linear mixed model expressing the temporal trend in SBP as a quadratic polynomial in time for each treatment. Student's t-test or Mann-Whitney rank-sum test was performed as appropriate for 2-group comparisons. One or two-way ANOVA with Holm-Sidak post-hoc analyses were performed for multiple-group and multiple-manipulation analysis. Fisher's exact probability test was used to determine differences between groups in the incidence of aneurysm formation and in mortality due to rupture. Values of $P<0.05$ were considered statistically significant.

Results

AngII Infusion Increased Hippo-YAP Signaling Proteins in Ascending and Abdominal Aortas

To examine the effect of AngII on Hippo-YAP signaling in the aorta, male C57BL/6J mice were infused with saline or AngII (1,000 ng/kg/min) via osmotic mini-pumps for 7 days. Western blot analyses of ascending and abdominal

Table. Characteristics of the Study Group

	AngII+HFD	AngII+XMU-MP-1+HFD
N	13	14
SBP (mmHg)		
Baseline	151±3	150±2
Day 28	184±4*	178±4*
BW (g)		
Baseline	22.5±0.8	23.2±0.7
Day 28	25.6±0.6	26.1±0.6
T-Cho (mg/dL)	995±62	926±62

Data are presented as mean±SEM. AngII, angiotensin II; HFD, high fat diet; XMU-MP-1, 4-((5,10-dimethyl-6-oxo-6,10-dihydro-5H-pyrimido[5,4-b] thieno[3,2-e] [1,4]diazepin-2-yl)amino) benzenesulfonamide; SBP, systolic blood pressure; BW, body weight; T-Cho, total cholesterol concentration. *P<0.05 vs. baseline.
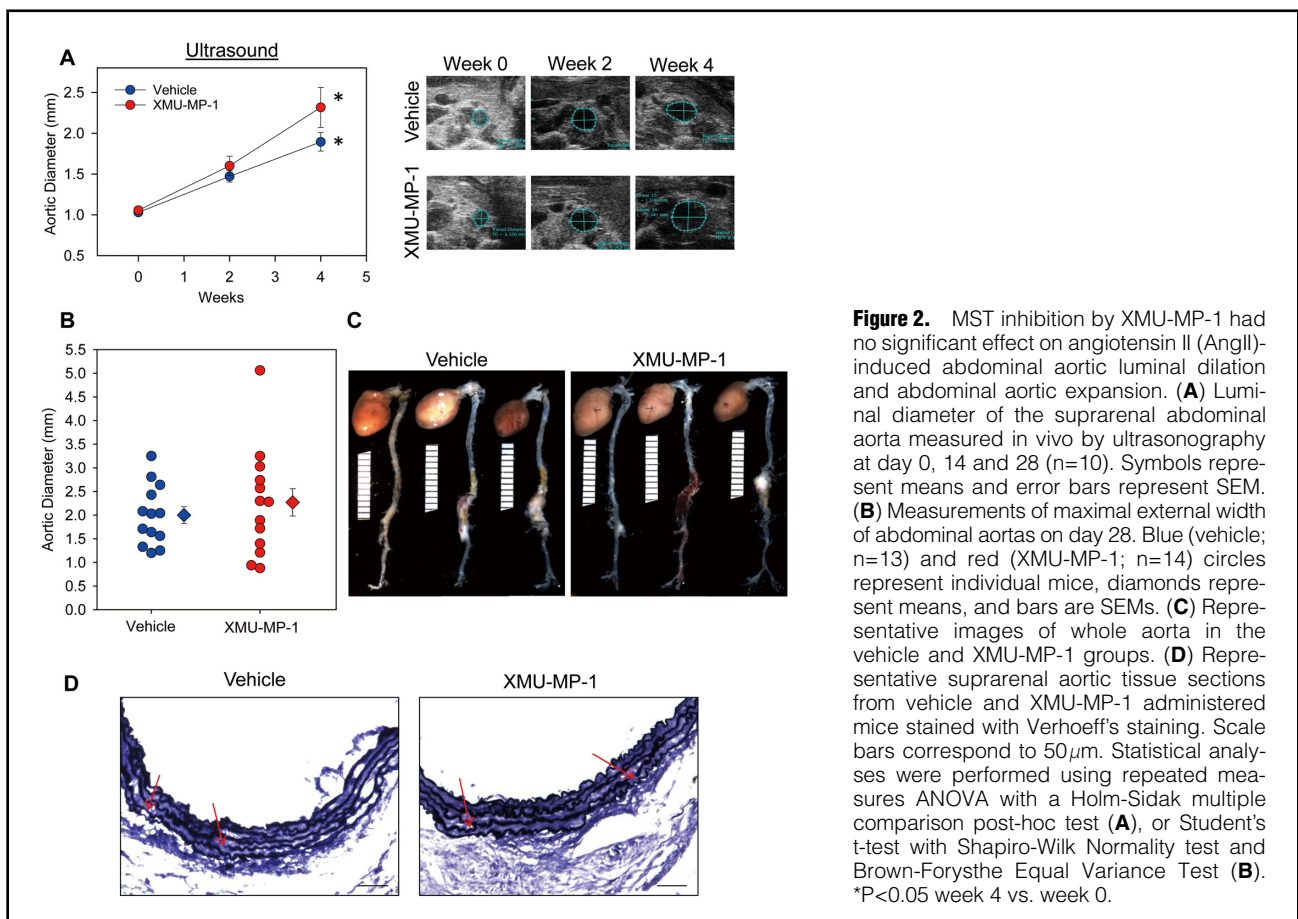

Figure 2. MST inhibition by XMU-MP-1 had no significant effect on angiotensin II (AngII)-induced abdominal aortic luminal dilation and abdominal aortic expansion. (**A**) Luminal diameter of the suprarenal abdominal aorta measured in vivo by ultrasonography at day 0, 14 and 28 (n=10). Symbols represent means and error bars represent SEM. (**B**) Measurements of maximal external width of abdominal aortas on day 28. Blue (vehicle; n=13) and red (XMU-MP-1; n=14) circles represent individual mice, diamonds represent means, and bars are SEMs. (**C**) Representative images of whole aorta in the vehicle and XMU-MP-1 groups. (**D**) Representative suprarenal aortic tissue sections from vehicle and XMU-MP-1 administered mice stained with Verhoeff's staining. Scale bars correspond to 50 μm. Statistical analyses were performed using repeated measures ANOVA with a Holm-Sidak multiple comparison post-hoc test (**A**), or Student's t-test with Shapiro-Wilk Normality test and Brown-Forysthe Equal Variance Test (**B**). *P<0.05 week 4 vs. week 0.

aortas showed a significant increase in MST1, p-MST1, p-MOB, p-YAP, TAZ and YAP proteins with AngII infusion, compared to saline controls (**Figure 1A,B**). However, AngII infusion showed a significant striking increase in MST1, p-MOB, p-YAP, and YAP proteins in the ascending aorta compared to the abdominal aorta (**Figure 1A,B**). Interestingly, the ratio of p-YAP/t-YAP is not significantly different upon AngII infusion compared to saline controls. In addition, immunofluorescent staining of ascending aortas from 28 days AngII-infused mice showed increased positive staining of YAP (**Figure 1C**) and p-YAP (**Supplementary Figure 1A**) proteins, especially in the aortic medial layer. In addition, higher magnification images showed YAP-positive staining areas are co-localized with aortic medial nuclei (**Figure 1C**). Similarly, immunohistochemical staining of abdominal aortic aneurysmal sections from 28 days AngII-infused LDL receptor −/− mice fed with a western diet showed a strong positive staining for both YAP and p-YAP proteins (**Figure 1D**, **Supplementary Figure 1B**).

Pharmacological Inhibition of MST1/2 Suppresses AngII-Induced Ascending AAs

In order to understand whether the activated/increased Hippo-YAP signaling proteins have any role in AngII-induced ascending and abdominal aortic aneurysmal development, we utilized the pharmacological inhibitor, XMU-MP-1, to inhibit the scaffolding protein, MST1/2. Based on the literature,[13,14,23] we tested the effect of XMU-MP-1 at the dose of 3mg/kg/day on aortic MST-1 phosphorylation in mice. Male LDL receptor −/− mice were fed with a western diet for 2 weeks. To inhibit Hippo-YAP signaling, mice were administered with either vehicle or XMU-MP-1 at the dose of 3mg/kg/day by gavage for 2 weeks. After 1 week of western diet and drug administration, mice were infused with AngII (1,000 ng/kg/min) via osmotic mini-pumps for 7 days. Western blot analyses of ascending aortas showed a significant increase in p-MST1 and total MST1, with AngII infusion, compared to saline controls (**Supplementary Figure 2**). However, XMU-MP-1 administration completely suppressed MST-1 phosphorylation with a moderate effect on total MST-1 (**Supplementary Figure 2**). Based on the strong effect of XMU-MP-1 on AngII-induced MST-1 phosphorylation, we utilized the 3mg/kg/day dose of XMU-MP-1 for the subsequent aneurysmal studies.

For aortic aneurysmal studies, male LDL receptor −/− mice were fed with a western diet for 5 weeks. To inhibit Hippo-YAP signaling, mice were administered with either vehicle or XMU-MP-1 at the dose of 3mg/kg/day by gavage for 5 weeks. After 1 week of a western diet and drug administration, mice were infused with AngII (1,000 ng/kg/min) for 4 weeks. Mice were continued on a western diet and pharmacological inhibitor or vehicle throughout AngII infusion.

AngII infusion for 28 days significantly increased SBP compared to baseline in both vehicle and XMU-MP-1 administered groups of LDL receptor −/− mice (**Table**). Administration of XMU-MP-1 did not have an effect on body weight and plasma total cholesterol concentrations (**Table**). AngII infusion significantly, but equivalently increased luminal dilation of abdominal aortas in both vehicle and XMU-MP-1 administered groups, as measured by ultrasound on days 0,14 and 28 (Vehicle: Day 0 – 1.03±0.03, Day 14 – 1.47±0.06, Day 28 – 1.89±0.11; XMU-MP-1: Day 0 – 1.05±0.04, Day 7 – 1.60±0.11, Day 28 – 2.31±0.24;
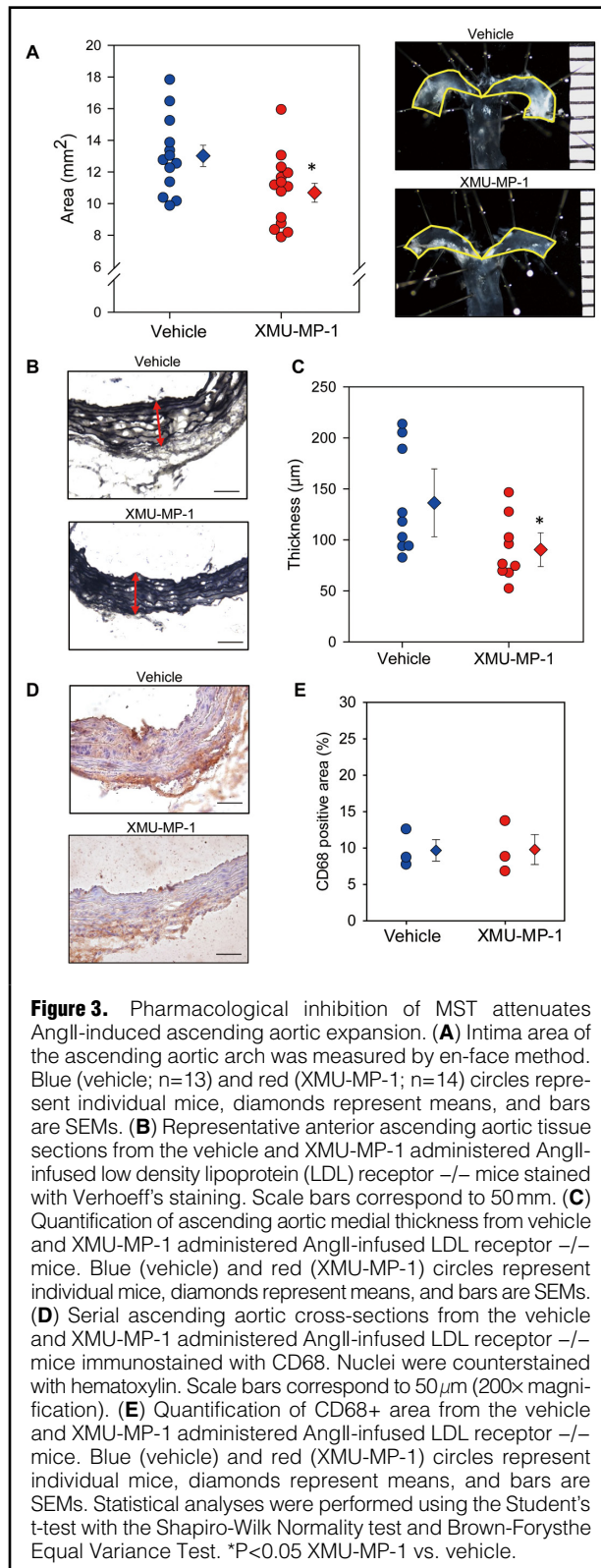

Figure 3. Pharmacological inhibition of MST attenuates AngII-induced ascending aortic expansion. (**A**) Intima area of the ascending aortic arch was measured by en-face method. Blue (vehicle; n=13) and red (XMU-MP-1; n=14) circles represent individual mice, diamonds represent means, and bars are SEMs. (**B**) Representative anterior ascending aortic tissue sections from the vehicle and XMU-MP-1 administered AngII-infused low density lipoprotein (LDL) receptor −/− mice stained with Verhoeff's staining. Scale bars correspond to 50 mm. (**C**) Quantification of ascending aortic medial thickness from vehicle and XMU-MP-1 administered AngII-infused LDL receptor −/− mice. Blue (vehicle) and red (XMU-MP-1) circles represent individual mice, diamonds represent means, and bars are SEMs. (**D**) Serial ascending aortic cross-sections from the vehicle and XMU-MP-1 administered AngII-infused LDL receptor −/− mice immunostained with CD68. Nuclei were counterstained with hematoxylin. Scale bars correspond to 50 μm (200× magnification). (**E**) Quantification of CD68+ area from the vehicle and XMU-MP-1 administered AngII-infused LDL receptor −/− mice. Blue (vehicle) and red (XMU-MP-1) circles represent individual mice, diamonds represent means, and bars are SEMs. Statistical analyses were performed using the Student's t-test with the Shapiro-Wilk Normality test and Brown-Forsythe Equal Variance Test. *P<0.05 XMU-MP-1 vs. vehicle.

P=NS, **Figure 2A,B**). In addition, administration of XMU-MP-1 had no influence on AngII-induced AAA formation (**Figure 2C**), as measured by external aortic width expansion (Mean width; Vehicle: 2.00±0.18 mm vs. XMU-MP-1: 2.27±0.29 mm, P=NS). Verhoeff's staining of abdominal
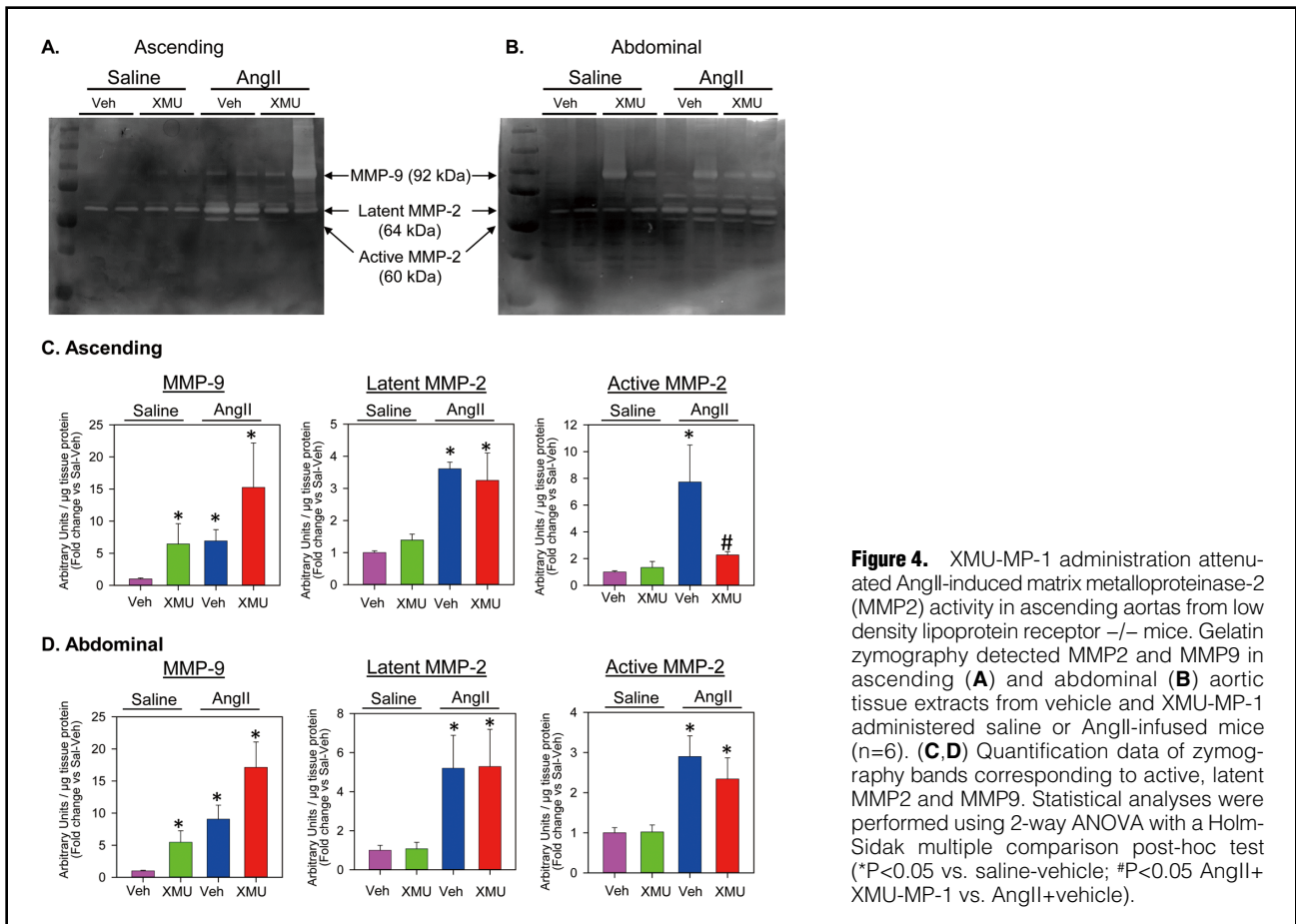
Figure 4. XMU-MP-1 administration attenuated AngII-induced matrix metalloproteinase-2 (MMP2) activity in ascending aortas from low density lipoprotein receptor −/− mice. Gelatin zymography detected MMP2 and MMP9 in ascending (**A**) and abdominal (**B**) aortic tissue extracts from vehicle and XMU-MP-1 administered saline or AngII-infused mice (n=6). (**C,D**) Quantification data of zymography bands corresponding to active, latent MMP2 and MMP9. Statistical analyses were performed using 2-way ANOVA with a Holm-Sidak multiple comparison post-hoc test (*P<0.05 vs. saline-vehicle; #P<0.05 AngII+ XMU-MP-1 vs. AngII+vehicle).

aortic sections revealed the occurrence of focal aortic medial elastin layer disruption (**Figure 2D**) with AngII infusion in both vehicle and XMU-MP-1 groups. Furthermore, XMU-MP-1 administration had no effect on AngII-induced atherosclerotic lesion areas in aortic arches (Percent Lesion: Vehicle: 4.61±1.38 vs. 6.57±1.76; n=13–14, P=NS, **Supplementary Figure 3**).

Next, we examined the effect of XMU-MP-1 administration on the AngII-induced ascending AA formation. Dilation of the ascending aortas was determined by measuring intimal area of the ascending aorta. XMU-MP-1 administration significantly attenuated AngII-induced ascending aortic dilation compared to vehicle administered groups (Area; Vehicle: 13.0±0.67mm² vs. XMU-MP-1: 10.8±0.60mm², P=0.022, Student's t-test, **Figure 3A**).

Pharmacological Inhibition of MST1/2 Suppressed AngII-Induced Aortic Medial Thickness in the Ascending Aorta

Histology (Verhoeff's staining) and CD68 immunostaining on ascending aortic sections showed the occurrence of focal elastin disruption (**Figures 3B,C**) associated with CD68+ macrophage accumulation (**Figures 3D,E**). In addition, AngII infusion increased ascending aortic medial thickness (**Figure 3B,C**), as measured from the inner to outer elastic lamina. As reported earlier, Verhoeff's staining showed that increased aortic medial thickness is associated with an expansion of intraelastic spaces towards the adventitial aspect of the media (**Figure 3B,C**). Administration of XMU-MP-1 significantly attenuated AngII-induced

medial thickness (P<0.05; **Figure 3B,C**) in the ascending aortas of LDL receptor −/− mice. Quantification of CD68+ macrophage staining revealed that XMU-MP-1 administration had no effect on accumulation of infiltrated macrophages in the AngII-infused aortas (**Figure 3D,E, Supplementary Figure 4**). Furthermore, quantification of DAPI-stained nuclei revealed that XMU-MP-1 had no effect on AngII-induced hyperplasia in the ascending aorta (**Supplementary Figure 5**).

MST1/2 Inhibition Attenuated AngII-Induced MMP-2 Activation in Ascending Aortas

Activation of matrix metalloproteinases (MMPs) has been shown to play an associative role in the progression of AAs in mice, mainly by mediating elastin and other extracellular matrix protein degradation. Because we observed a reduction in AngII-induced ascending aortic medial thickness along with preserved medial elastin layer with XMU-MP-1 administration, we next sought to determine the effect of XMU-MP-1 administration on AngII-induced MMP activity in the ascending aortas. Male LDL receptor −/− mice on a western diet were administered with either vehicle or XMU-MP-1 (3 mg/kg/day) by gavage for 2 weeks. After 1 week of a western diet and drug administration, mice were infused with AngII (1,000 ng/kg/min) for 7 days. AngII-infusion significantly increased aortic MMP-2 and MMP-9 activity in both ascending and abdominal aortas, as analyzed by gelatin-in-gel zymography. Interestingly, XMU-MP-1 administration significantly suppressed

AngII-induced active MMP-2 but not latent MMP-2 only in the ascending aorta (**Figure 4A–C**).

Discussion

AngII infusion into LDL receptor −/− mice is a well-established model of generating ascending and abdominal AAs. In this present study, we demonstrated that pharmacological inhibition of MST-1/2 signaling attenuates the development of AngII-induced ascending not abdominal AAs in male LDL receptor −/− mice. The protective effect of MST1/2 inhibition was associated with the reduction of ascending aortic medial degradation and gelatinase-mediated extracellular matrix degradation in the aorta. This study strongly supports the hypothesis that the underlying mechanism in the development of ascending AA is uniquely different from abdominal AAs.

In this present study, AngII infusion profoundly increased Hippo-YAP signaling proteins[7–9] such as MST1, p-MOB, P-YAP, and YAP in both ascending and abdominal aortas; however, the magnitude of the increase is significantly higher in the ascending aorta compared to the abdominal aorta. This finding is supported by an earlier study that demonstrated that smooth muscle cells (SMCs) harvested from β-amino propionitrile (BAPN)-induced dissected rat aortas had elevated MST-1 and p-YAP proteins.[24] Interestingly, in our study, AngII infusion significantly increased both total and p-YAP in the aortas, which is quite unusual in that the classical Hippo-YAP signaling activation resulted in activated p-YAP with a reduction in total YAP protein. In contrast, in human aortic endothelial cells, Wang et al reported that AngII stimulation suppressed total YAP and increased p-YAP, as observed in other diseased conditions.[25] The contrary observation of increased total and p-YAP in our present study could be due to a SMC-specific YAP regulation by AngII. In support of our observation, an earlier study by Lin et al demonstrated that AngII infusion increased both total and phospho-YAP in the right common carotid artery in hypertensive rats and cultured rat thoracic aorta SMCs via AT1R activation.[26] Interestingly, Lin et al also reported that the p-YAP/t-YAP ratio was decreased in AngII-infused carotid arteries.[26] However, in our present study, we did not observe any significant difference in the p-YAP/t-YAP ratio in AngII-infused aortas. The one possible explanation could be due to differences in the phenotypic response of medial SMCs of different embryonic origins presented in aortic media vs. carotid arteries.[27] However, further side-by-side comparison studies using both aortic and carotid endothelial and SMCs are warranted to explain the regulation of YAP by AngII in the vessel wall. In addition, the dysregulated YAP protein has been observed in the ascending aorta of Marfan syndrome patients.[12] However, no information is available on the regulation of Hippo-YAP signaling in abdominal aortic aneurysmal patients currently. Activated MST1 has been shown to promote cellular apoptosis, which in turn leads to a decrease in tissue cell number and organ atrophy.[28,29] Consistently, in our present study, AngII infusion showed dramatic destruction of the ascending aortic media, which is highly rich in SMCs. The observed beneficial effect of XMU-MP-1 administration on AngII-induced ascending aortic dilation is possibly due to its effect on MST1 signaling inhibition and thereby preventing aortic SMC loss and degradation.

XMU-MP-1 administration attenuated AngII-induced aortic medial destruction in the ascending aorta. In agreement with previous studies, AngII-induced medial destruction was associated with the accumulation of CD68+ macrophages throughout the intralamellar spaces on the adventitial site of the vessel wall.[16,21] The beneficial effect of XMU-MP-1 on the attenuation of elastin fiber destruction in the aortic media is mainly due to its effect on the suppression of AngII-induced matrix metalloproteinases-2 (MMP2) production by infiltrated macrophages in the ascending aorta. In support, our present data clearly suggested that XMU-MP-1 administration had no effect on AngII-induced macrophage infiltration into the ascending aortic medial layer or the total number of nuclei in the ascending aortic media, whereas it preserved or protected AngII-induced aortic medial destruction. These data suggest that XMU-MP-1 may exert its beneficial effect by suppressing MMP production or secretion by infiltrated macrophages into the aortic media. However, our current study does not explain the mechanism by which XMU-MP-1 administration mediated MST-1 inhibition suppressed AngII-induced MMP-2 activity. AngII is known to induce MMP-2 activity by activating various signaling cascades such as ERK signaling, JNK/STAT-3 pathway, reactive oxygen species (e.g., P47 phox), etc.[30–32] One possible explanation for the observed reduction in AngII-induced aortic MMP-2 activity with XMU-MP-1 administration could be due to the suppressive effect of XMU-MP-1 on AngII-induced MST-1. In support, transgenic mice overexpressing cardiac-specific dominant negative MST-1 resulted in suppression of myocardial infarction-induced MMP2 in heart tissues.[33] However, it is not clear by which mechanisms MST-1 activation promotes MMP-2 activity currently. In addition, XMU-MP-1 has been shown to suppress MMP-9 in mice after subarachnoid hemorrhage injury by influencing NFkB signaling.[23] Further studies are warranted to explore Hippo-YAP signaling molecules' potential interaction, especially MST-1 and YAP, with the known AngII-induced signaling cascades that mediate AngII-induced MMP-2 activity. However, to our knowledge, this is the first report to examine and demonstrate the suppressive effect of XMU-MP-1 on AngII-induced MMP2 activity in the aorta.

One possible explanation for the differential effect of XMU-MP-1 on AngII-induced ascending and abdominal AAs could be due to the differential expression of Hippo-YAP signaling molecules by aortic SMCs of differential embryonic origin between the ascending and abdominal aortas. The aortic SMCs of the ascending aorta consist of SMCs originated from the second heart field and cardiac neural crest, whereas the SMCs in the abdominal aorta originated from splanchnic mesoderm.[34,35] In our study, compared to the abdominal aorta, ascending aortas expresses 2-fold higher Hippo-YAP proteins upon AngII infusion, which in turn speculatively suggests that SMCs of the second heart field or cardiac neural crest origin and/or adventitial fibroblasts/ endothelial cells in the ascending aorta activates and promotes higher Hippo-YAP proteins in response to AngII compared to SMCs that originated from splanchnic mesoderm or adventitial fibroblasts / endothelial cells of abdominal aortas. However, further studies are warranted to test and understand these differential responses by utilizing the available MST1 floxed mice[36] and mice expressing Cre recombinase under the control of MEF2C or a CNC promoter.[35]

In conclusion, this study demonstrated for the first time

that inhibition of Hippo-YAP signaling by the MST1/2 inhibitor, XMU-MP-1, significantly attenuated the development of AngII-induced ascending aortic expansion in LDL receptor-deficient mice. Inhibition of Hippo-YAP might offer a new therapeutic target to prevent ascending aortic expansion. Further studies are warranted to determine the role of specific molecular components of Hippo-YAP signaling in the development of these AngII-induced vascular pathologies, which will require mice with genetic deficiency of specific key proteins of the Hippo-YAP pathway.

Acknowledgments

Disclosures

The authors report no conflicts of interest.

IRB Information

This study was approved by the University of Kentucky Institutional Animal Care and Use Committee (Protocol # 2011-0907).

References

1. Pinard A, Jones GT, Milewicz DM. Genetics of thoracic and abdominal aortic diseases. *Circ Res* 2019; **124:** 588–606.
2. Quintana RA, Taylor WR. Cellular mechanisms of aortic aneurysm formation. *Circ Res* 2019; **124:** 607–618.
3. Saeyeldin AA, Velasquez CA, Mahmood SUB, Brownstein AJ, Zafar MA, Ziganshin BA, et al. Thoracic aortic aneurysm: Unlocking the "silent killer" secrets. *Gen Thorac Cardiovasc Surg* 2019; **67:** 1–11.
4. Sakalihasan N, Michel JB, Katsargyris A, Kuivaniemi H, Defraigne JO, Nchimi A, et al. Abdominal aortic aneurysms. *Nat Rev Dis Primers* 2018; **4:** 34.
5. Okuyama M, Uchida HA, Hada Y, Kakio Y, Otaka N, Umebayashi R, et al. Exogenous vasohibin-2 exacerbates angiotensin II-induced ascending aortic dilation in mice. *Circ Rep* 2019; **1:** 155–161.
6. Kurosawa K, Matsumura JS, Yamanouchi D. Current status of medical treatment for abdominal aortic aneurysm. *Circ J* 2013; **77:** 2860–2866.
7. Chen X, Li Y, Luo J, Hou N. Molecular mechanism of Hippo-YAP1/TAZ pathway in heart development, disease, and regeneration. *Front Physiol* 2020; **11:** 389.
8. Zheng Y, Pan D. The Hippo signaling pathway in development and disease. *Dev Cell* 2019; **50:** 264–282.
9. Wang J, Liu S, Heallen T, Martin JF. The Hippo pathway in the heart: Pivotal roles in development, disease, and regeneration. *Nat Rev Cardiol* 2018; **15:** 672–684.
10. Bai H, Zhang N, Xu Y, Chen Q, Khan M, Potter JJ, et al. Yes-associated protein regulates the hepatic response after bile duct ligation. *Hepatology* 2012; **56:** 1097–1107.
11. Gao T, Zhou D, Yang C, Singh T, Penzo-Mendez A, Maddipati R, et al. Hippo signaling regulates differentiation and maintenance in the exocrine pancreas. *Gastroenterology* 2013; **144:** 1543–1553, 1553.e1.
12. Li H, Jiang W, Ren W, Guo D, Guo J, Wang X, et al. Down-regulation of the Yes-associated protein is associated with extracellular matrix disorders in ascending aortic aneurysms. *Stem Cells Int* 2016; **2016:** 6786184.
13. Fan F, He Z, Kong LL, Chen Q, Yuan Q, Zhang S, et al. Pharmacological targeting of kinases MST1 and MST2 augments tissue repair and regeneration. *Sci Transl Med* 2016; **8:** 352ra108.
14. Triastuti E, Nugroho AB, Zi M, Prehar S, Kohar YS, Bui TA, et al. Pharmacological inhibition of Hippo pathway, with the novel kinase inhibitor XMU-MP-1, protects the heart against adverse effects during pressure overload. *Br J Pharmacol* 2019; **176:** 3956–3971.
15. Howatt DA, Balakrishnan A, Moorleghen JJ, Muniappan L, Rateri DL, Uchida HA, et al. Leukocyte calpain deficiency reduces angiotensin II-induced inflammation and atherosclerosis but not abdominal aortic aneurysms in mice. *Arterioscler Thromb Vasc Biol* 2016; **36:** 835–845.
16. Subramanian V, Moorleghen JJ, Balakrishnan A, Howatt DA, Chishti AH, Uchida HA. Calpain-2 compensation promotes angiotensin II-induced ascending and abdominal aortic aneurysms in calpain-1 deficient mice. *PLoS One* 2013; **8:** e72214.
17. Subramanian V, Uchida HA, Ijaz T, Moorleghen JJ, Howatt DA, Balakrishnan A. Calpain inhibition attenuates angiotensin II-induced abdominal aortic aneurysms and atherosclerosis in low-density lipoprotein receptor-deficient mice. *J Cardiovasc Pharmacol* 2012; **59:** 66–76.
18. Daugherty A, Rateri D, Hong L, Balakrishnan A. Measuring blood pressure in mice using volume pressure recording, a tail-cuff method. *J Vis Exp* 2009; **15:** 1291.
19. Subramanian V, Golledge J, Ijaz T, Bruemmer D, Daugherty A. Pioglitazone-induced reductions in atherosclerosis occur via smooth muscle cell-specific interaction with PPAR{gamma}. *Circ Res* 2010; **107:** 953–958.
20. Daugherty A, Cassis LA. Mouse models of abdominal aortic aneurysms. *Arterioscler Thromb Vasc Biol* 2004; **24:** 429–434.
21. Rateri DL, Moorleghen JJ, Balakrishnan A, Owens AP, 3rd, Howatt DA, Subramanian V, et al. Endothelial cell-specific deficiency of Ang II type 1a receptors attenuates Ang II-induced ascending aortic aneurysms in LDL receptor−/− mice. *Circ Res* 2011; **108:** 574–581.
22. Muniappan L, Javidan A, Jiang W, Mohammadmoradi S, Moorleghen JJ, Katz WS, et al. Calpain inhibition attenuates adipose tissue inflammation and fibrosis in diet-induced obese mice. *Sci Rep* 2017; **7:** 14398.
23. Qu J, Zhao H, Li Q, Pan P, Ma K, Liu X, et al. MST1 suppression reduces early brain injury by inhibiting the NF-kappaB/MMP-9 pathway after subarachnoid hemorrhage in mice. *Behav Neurol* 2018; **2018:** 6470957.
24. Shi Y, Liu B, Wang CS, Yang CS. MST1 down-regulation in decreasing apoptosis of aortic dissection smooth muscle cell apoptosis. *Eur Rev Med Pharmacol Sci* 2018; **22:** 2044–2051.
25. Wang X, Zhang H, Ge Y, Liu J, Rong D, Cao L, et al. Angiotensin type 1 receptor regulates yes-associated protein in vascular endothelial cells. *Exp Ther Med* 2020; **19:** 748–754.
26. Lin M, Yuan W, Su Z, Lin C, Huang T, Chen Y, et al. Yes-associated protein mediates angiotensin II-induced vascular smooth muscle cell phenotypic modulation and hypertensive vascular remodelling. *Cell Prolif* 2018; **51:** e12517.
27. Majesky MW. Vascular smooth muscle diversity: Insights from developmental biology. *Curr Atheroscler Rep* 2003; **5:** 208–213.
28. Wang P, Mao B, Luo W, Wei B, Jiang W, Liu D, et al. The alteration of Hippo/YAP signaling in the development of hypertrophic cardiomyopathy. *Basic Res Cardiol* 2014; **109:** 435.
29. Ikeda S, Sadoshima J. Regulation of myocardial cell growth and death by the Hippo pathway. *Circ J* 2016; **80:** 1511–1519.
30. Wang C, Qian X, Sun X, Chang Q. Angiotensin II increases matrix metalloproteinase 2 expression in human aortic smooth muscle cells via AT1R and ERK1/2. *Exp Biol Med (Maywood)* 2015; **240:** 1564–1571.
31. Kopaliani I, Martin M, Zatschler B, Bortlik K, Muller B, Deussen A. Cell-specific and endothelium-dependent regulations of matrix metalloproteinase-2 in rat aorta. *Basic Res Cardiol* 2014; **109:** 419.
32. Luchtefeld M, Grote K, Grothusen C, Bley S, Bandlow N, Selle T, et al. Angiotensin II induces MMP-2 in a p47phox-dependent manner. *Biochem Biophys Res Commun* 2005; **328:** 183–188.
33. Odashima M, Usui S, Takagi H, Hong C, Liu J, Yokota M, et al. Inhibition of endogenous Mst1 prevents apoptosis and cardiac dysfunction without affecting cardiac hypertrophy after myocardial infarction. *Circ Res* 2007; **100:** 1344–1352.
34. Majesky MW. Developmental basis of vascular smooth muscle diversity. *Arterioscler Thromb Vasc Biol* 2007; **27:** 1248–1258.
35. Sawada H, Rateri DL, Moorleghen JJ, Majesky MW, Daugherty A. Smooth muscle cells derived from second heart field and cardiac neural crest reside in spatially distinct domains in the media of the ascending aorta: Brief report. *Arterioscler Thromb Vasc Biol* 2017; **37:** 1722–1726.
36. Lu L, Li Y, Kim SM, Bossuyt W, Liu P, Qiu Q, et al. Hippo signaling is a potent in vivo growth and tumor suppressor pathway in the mammalian liver. *Proc Natl Acad Sci USA* 2010; **107:** 1437–1442.

Supplementary Files

Please find supplementary file(s);
http://dx.doi.org/10.1253/circrep.CR-20-0104